NONLINEAR SAW PROPAGATION IN THIN-FILM SYSTEMS WITH RESIDUAL STRESS*

R. E. Kumon†
National Institute of Standards and Technology (NIST), 325 Broadway, Boulder, Colorado 80305–3328, U.S.A.

Abstract— The propagation of small- and finite-amplitude surface acoustic waves (SAWs) in stressed thin-film systems is modeled. Results are presented for an initially monofrequency, plane wave traveling in the $\langle 100 \rangle$ direction of systems composed of either Ge (loading) or diamond (stiffening) epitaxial films under compressive stress on an unstressed (001) Si substrate. Cases are considered for both thinner and thicker films in terms of their ratios of dispersion to nonlinearity ratios. For finite-amplitude waves, comparison between unstressed and stressed films indicates that larger effects occur at longer propagation distances and for higher harmonics.

I. INTRODUCTION AND MOTIVATION

The thin-film deposition process can create large residual stresses that change the film's effective mechanical properties and therefore its performance in a product. Measurements of small-amplitude SAWs can characterize stresses through the acoustoelastic effect on the velocity dispersion. Finite-amplitude SAWs, which nonlinearly generate harmonics as they propagate, may be more sensitive to stress because the combined effects of the nonlinearity and dispersion are cumulative with distance. This study compares the relative magnitudes of calculated stress-induced changes for small- and finite-amplitude SAWs.

II. THEORY

Assume that a small-amplitude, plane SAW is propagating in the x_1 direction. Its propagation in an in-plane equibiaxially stressed, anisotropic thin-film system is described by the linear equation [1], [2]

$$C^{\text{eff}}_{ijkl}\frac{\partial^2 u_k}{\partial x_j \partial x_l} + \sigma^{\text{res}}\frac{\partial^2 u_i}{\partial x_1^2} = \rho^{\text{eff}}\frac{\partial^2 u_i}{\partial t^2}\,, \qquad (1)$$

where x_i are Lagrangian coordinates (i = 1,2,3), t is time, u_i are the SAW particle displacement components, and σ^{res} is the residual stress. The effective elastic constants and density are given by

$$\begin{aligned} C^{\text{eff}}_{ijkl} &= C_{ijkl}(1 - \Delta e^{\text{res}} + e^{\text{res}}_{ii} + e^{\text{res}}_{jj} + \\ &\quad e^{\text{res}}_{kk} + e^{\text{res}}_{ll}) + C_{ijklmn}e^{\text{res}}_{mn}\,, \qquad (2) \\ \rho^{\text{eff}} &= \rho(1 - \Delta e^{\text{res}})\,, \qquad (3) \end{aligned}$$

where $\Delta e^{\text{res}} = e^{\text{res}}_{11} + e^{\text{res}}_{22} + e^{\text{res}}_{33}$ is the linear volume dilatation due to residual strain, and C_{ijkl}, C_{ijklmn}, and ρ are, respectively, the unstressed second- and third-order elastic constants and density. A Green's function method [3] is used to compute the dispersion relations, subject to the boundary conditions specified in [2].

Propagation of finite-amplitude SAWs of the form

$$v_i(x_1, x_3, \tau) = \sum_{n=1}^{\infty} v_n(x_1)u_{ni}(x_3)e^{-in\omega\tau} + \text{ c.c.} \quad (4)$$

in the same systems can be described by the coupled spectral evolution equations [4], [5]

$$\frac{dv_n}{dx_1} + (\alpha_n + i\delta_n)v_n = \frac{n^2\omega}{2\rho c^4}\sum_{l+m=n}\frac{lm}{|lm|}S_{lm}v_l v_m\,, \qquad (5)$$

where v_i are the ith particle velocity components, u_{ni} describe the depth dependence of the nth harmonic component, v_n are the nth harmonic components, α_n and δ_n are, respectively, the attenuation and dispersion coefficients of v_n, ω is the fundamental angular frequency, and c is the SAW velocity. S_{lm} is a nonlinearity matrix characterizing the coupling of the lth and mth harmonic to generate the $n(= l + m)$th harmonic and accounts for terms up to quadratic order in strain in the constitutive equation. The only effect of the film is to cause dispersion among the harmonics generated in the substrate. This assumption is valid provided that the film is thin compared to the wavelengths of the dominant harmonics, so that the depth profiles of the linearized solution are only negligibly perturbed [5]. All cases considered here satisfy this criterion.

A dimensionless parameter that characterizes the ratio of dispersion to nonlinearity can be constructed [5]

in the form

$$D = \frac{(dc/df)_0 f}{\beta v}, \tag{6}$$

where $(dc/df)_0$ is the slope of the dispersion curve at zero frequency, $\beta = -4S_{11}/\rho c^2$ is the nonlinearity coefficient [6], and f and v are the characteristic frequency and particle velocity magnitude of the nonlinear SAW. Results are compared below for values of D corresponding to different film thicknesses less than 100 nm. With thicker films, the assumption of harmonic generation only in the substrate becomes harder to satisfy. In addition, thicker films tend to have less homogeneous and lower average residual stresses.

III. Results

A monofrequency source is assumed with fundamental frequency $f = 30$ MHz and peak acoustic particle velocity $v = 50$ m/s (peak acoustic strain of 0.01), values that are the same order of magnitude as those in recent experiments [7]. With $\beta = -0.12$ for the chosen cut and direction, these values result in a characteristic length scale for nonlinear distortion of $x_0 = 20$ mm [6]. The unstressed densities of Si, Ge, and diamond are taken as 2329 kg/m^3, 5323 kg/m^3, and 3512 kg/m^3, respectively. Unstressed elastic constant data are taken from [8], [9], [10].

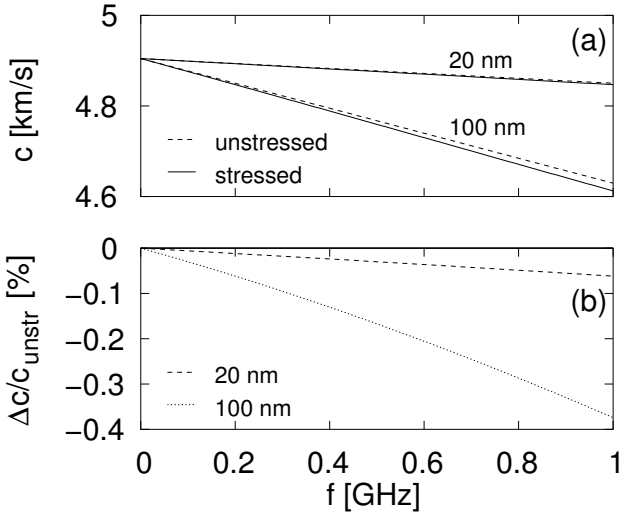

Figure 1: (a) Velocity and (b) fractional change in velocity as a function of frequency for 20 nm and 100 nm Ge films on Si (001) substrate along $\langle 001 \rangle$.

A. Ge films (loading)

Consider the case of Ge films loading a Si substrate shown in Figs. 1, 2, and 3. The dispersion relations for unstressed and stressed ($\sigma^{\rm res} = -5$ GPa) films of thicknesses of 20 nm and 100 nm, are shown in Fig. 1(a). As seen in Fig. 1(b), the fractional change in velocity $(c - c_{\rm unstr})/c_{\rm unstr}$ due to stress is less than -0.4 % even at the highest frequencies considered.

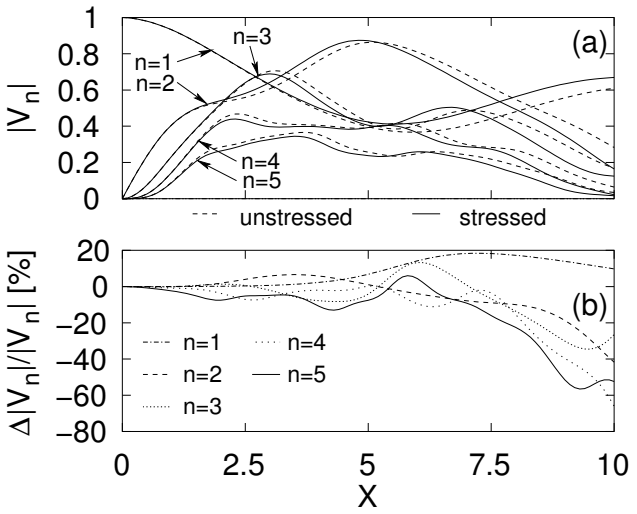

Figure 2: (a) Harmonic magnitudes and (b) their fractional change as a function of dimensionless propagation distance for 20 nm Ge film on Si (001) substrate along $\langle 001 \rangle$ for moderate dispersion.

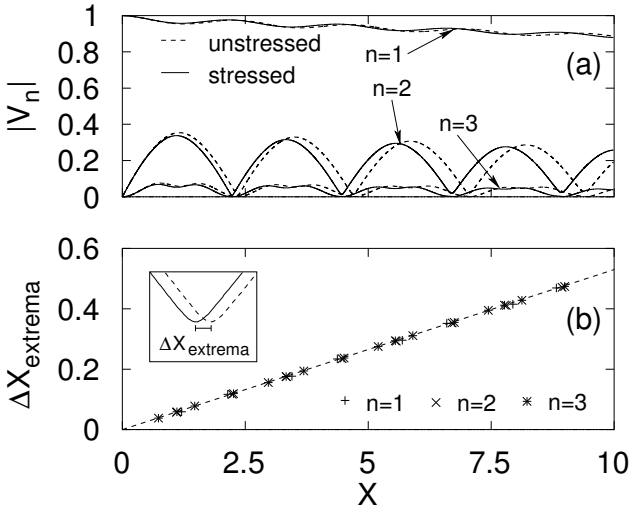

Figure 3: (a) Harmonic magnitudes and (b) extrema shifts as a function of dimensionless propagation distance for 100 nm Ge film on Si (001) substrate along $\langle 100 \rangle$ for strong dispersion.

For the 20 nm film, the slope of the dispersion curve in Fig. 1(a) yields $D = 0.26$, a moderate ratio of dispersion to nonlinearity [5]. Figures 2(a) and (b) show the magnitudes $|V_n|$ and the fractional change $(|V_n| - |V_n^{\rm unstr}|)/|V_n^{\rm unstr}|$, respectively, of the first five harmonic components $V_n = v_n/v_0$ as a function of the dimensionless propagation distance $X = x/x_0$. Observe that (1) the fractional change oscillates but generally increases in magnitude with propagation distance, and (2) the higher harmonics exhibit a relatively larger change than lower harmonics. Moreover, the fractional changes are greater than the fractional change in the SAW velocity shown in Fig. 1(b).

For the 100 nm film, $D = 1.3$, and the system exhibits strongly dispersive behavior [5] characterized by growth–decay cycles in the harmonic components seen in Fig. 3(a) for the first three harmonics. Again the effect of the stress is cumulative with distance as shown in Fig. 3(b) by the linear increase in the positions of the extrema $\Delta X_{\rm extrema} = |X_{\rm extrema}^{\rm str} - X_{\rm extrema}^{\rm unstr}|$ (see inset). Due to the higher dispersion, the harmonics experience a larger phase shift relative to each other and thus less efficient nonlinear coupling. Nevertheless, the fractional changes in the positions of the extrema increase linearly with distance by 5 % for every nonlinear length scale traversed. Like the 20 nm film, this effect is significantly larger than the small change in the fractional SAW velocity of Fig. 1(b).

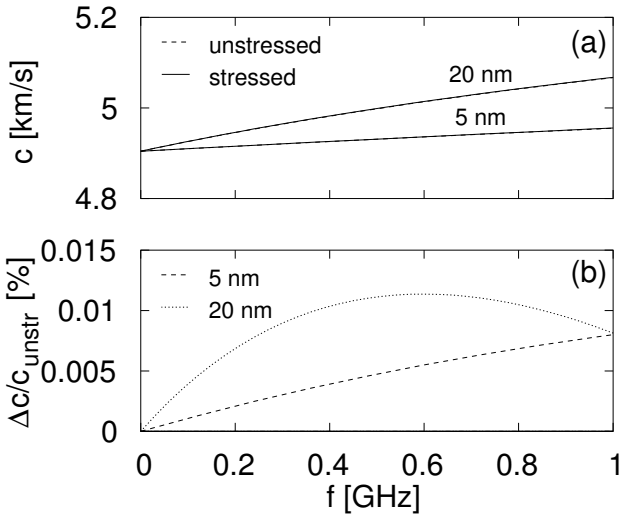

Figure 4: (a) Velocity and (b) fractional change in velocity as a function of frequency for 5 and 20 nm diamond films on Si (001) substrate along $\langle 100 \rangle$.

B. Diamond films (stiffening)

Next consider the case of diamond films stiffening a Si substrate shown in Figs. 4, 5, and 6. Because the difference between the SAW velocity $c_{\rm Si} = 4.90$ km/s and $c_{\rm diamond} = 11.0$ km/s is more than the difference between $c_{\rm Si}$ and $c_{\rm Ge} = 2.93$ km/s, thinner diamond films can achieve dispersion comparable to the Ge films in Sec. III-A. This effect can be seen in Fig. 4, which

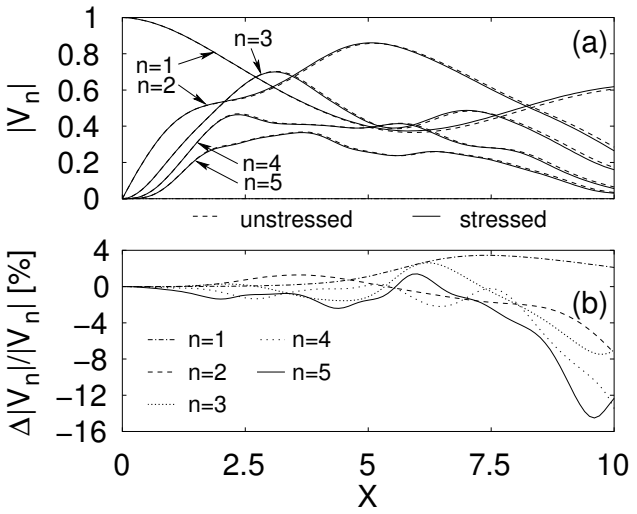

Figure 5: (a) Harmonic magnitudes and (b) their fractional change as a function of dimensionless propagation distance for 5 nm C film on Si (001) substrate along $\langle 100 \rangle$ for moderate dispersion.

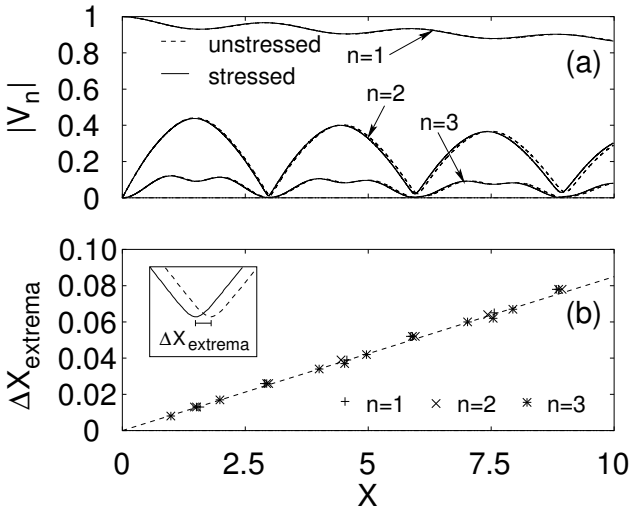

Figure 6: (a) Harmonic magnitudes and (b) extrema shifts as a function of dimensionless propagation distance for 20 nm C film on Si (001) substrate along $\langle 100 \rangle$ direction for strong dispersion.

shows the dispersion curves for unstressed and stressed ($\sigma^{\rm res} = -5$ GPa) films of thicknesses of 5 nm and 20 nm. Fig. 4(b) shows that the fractional velocity changes are considerably less as compared to Ge for the same amount of stress.

For the 5 nm film, $D = 0.23$ implies a moderate ratio of dispersion to nonlinearity. The evolution of the harmonics in Fig. 5 is qualitatively similar to evolution in the 20 nm Ge film in Fig. 2, but the fractional changes are less. This is partly due to the thinner film, which results in the SAW interacting less with stressed material. Despite the small values of $\Delta c/c$ in this case, there is still significant fractional change in the harmonic magnitudes.

For the 20 nm film, $D = 0.92$ implies strong dispersion and the growth–decay cycles in the harmonic components seen in Fig. 6. The resulting evolution is qualitatively similar to that for the 100 nm Ge film, although the magnitude of the extrema shift in Fig. 6(b) is less than in Fig 3(b).

IV. Conclusion

The propagation of initially monofrequency SAWs of small and finite amplitude is modeled in systems of residually stressed thin films with moderate and strong ratios of dispersion to nonlinearity . Even though the velocity dispersion between stressed and unstressed films in the Ge and diamond systems is only a fraction of a percent, the evolution of the harmonics is still affected significantly. The stress changes the magnitudes of the harmonics and the spatial period of the growth–decay cycles. Relatively larger changes occur at longer propagation distance and for the higher harmonics. Thinner diamond films give rise to dispersion of magnitude comparable to that of thicker Ge films, but the stress affects the dispersion less in the diamond films. The qualitative evolution of harmonics is similar in both materials. In summary, the evolution of the harmonic components of finite-amplitude SAWs can be quite sensitive to stress-induced dispersion, and may thus be a promising method for acoustically characterizing the residual stress of thin-film systems.

V. Acknowledgments

This work was performed while the author held a National Research Council Research Associateship Award at NIST. Thanks also to D. C. Hurley, V. K. Tewary, C. Flannery, and B. Yang.

VI. References

[1] Y.-H. Pao, W. Sachse, and H. Fukuoka, "Acoustoelasticity and ultrasonic measurements of residual stress," in *Physical Acoustics*, vol. 17, W. P. Mason and R. N. Thurston, Eds. New York: Academic Press, 1984, pp. 61–143.

[2] A. V. Osetrov, H. J. Frohlich, and R. Koch, "Acoustoelastic effect in anisotropic layered structures," *Phys. Rev. B*, vol. 62, pp. 13963–13969, Dec. 2000.

[3] V. K. Tewary, "Theory of elastic wave propagation in anisotropic film on anisotropic substrate: TiN film on single-crystal Si," *J. Acoust. Soc. Am.*, vol. 112, pp. 925–935, Sep. 2002.

[4] M. F. Hamilton, Yu. A. Il'inskii, and E. A. Zabolotskaya, "Nonlinear surface acoustic waves in crystals," *J. Acoust. Soc. Am.*, vol. 105, pp. 639–651, Feb. 1999.

[5] W.-S. Ohm, *Effects of Dispersion on Nonlinear Surface Acoustic Waves in Substrates Laminated with Films*, Ph.D. dissertation, The University of Texas at Austin, 2001.

[6] R. E. Kumon and M. F. Hamilton, "Directional dependence of nonlinear surface acoustic waves in the (001) plane of cubic crystals," *J. Acoust. Soc. Am.*, vol. 111, pp. 2060–2069, May 2002.

[7] A. M. Lomonosov, P. Hess, and A. P. Mayer, "Observation of solitary elastic surface pulses," *Phys. Rev. Lett.*, vol. 88, art. 076104, Feb. 2002.

[8] A. G. Every and A. K. McCurdy, "The elastic constants of crystals," in *Landolt-Börnstein, New Series*, vol. III/29a, D. F. Nelson, Ed. New York: Springer-Verlag, 1992, pp. 1–634.

[9] H. J. McSkimin and P. Andreatch, Jr., "Measurement of third-order moduli of silicon and germanium," *J. Appl. Phys.*, vol. 35, pp. 3312–3319, Nov. 1964.

[10] M. H. Grimsditch, E. Anastassakis, and M. Cardona, "Effect of uniaxial stress on the zone-center optical phonon of diamond," *Phys. Rev. B*, vol. 18, pp. 901–904, Jul. 1978.

†Email: kumon@boulder.nist.gov